Quaternary Research 81 (2014) 158–167

Contents lists available at ScienceDirect

Quaternary Research

journal homepage: www.elsevier.com/locate/yqres

Paleoclimate record in the Nubian Sandstone Aquifer, Sinai Peninsula, Egypt

Abdou Abouelmagd [a,b], Mohamed Sultan [a,*], Neil C. Sturchio [c], Farouk Soliman [b], Mohamed Rashed [b], Mohamed Ahmed [a,b], Alan E. Kehew [a], Adam Milewski [d], Kyle Chouinard [a]

[a] Department of Geosciences, Western Michigan University, Kalamazoo, MI 49008-5200, USA
[b] Department of Geology, Suez Canal University, Ismailia, 41522, Egypt
[c] Department of Earth and Environmental Sciences, University of Illinois at Chicago, Chicago, IL 60607-7059, USA
[d] Department of Geology, University of Georgia, Athens, GA 30602, USA

ARTICLE INFO

Article history:
Received 15 April 2013
Available online 4 December 2013

Keywords:
Paleoclimate
Nubian Sandstone Aquifer System (NSAS)
Sinai Peninsula
Noble gases
^{14}C adjusted model age
Paleowesterlies
Paleomonsoon

ABSTRACT

Sixteen groundwater samples collected from production wells tapping Lower Cretaceous Nubian Sandstone and fractured basement aquifers in Sinai were analyzed for their stable isotopic compositions, dissolved noble gas concentrations (recharge temperatures), tritium activities, and ^{14}C abundances. Results define two groups of samples: Group I has older ages, lower recharge temperatures, and depleted isotopic compositions (adjusted ^{14}C model age: 24,000–31,000 yr BP; δ^{18}O: −9.59‰ to −6.53‰; δ^{2}H: −72.9‰ to −42.9‰; <1 TU; and recharge T: 17.5–22.0°C) compared to Group II (adjusted ^{14}C model age: 700–4700 yr BP; δ^{18}O: −5.89‰ to −4.84‰; δ^{2}H: −34.5‰ to −24.1‰; <1 to 2.78 TU; and recharge T: 20.6–26.2°C). Group II samples have isotopic compositions similar to those of average modern rainfall, with larger d-excess values than Group I waters, and locally measurable tritium activity (up to 2.8 TU). These observations are consistent with (1) the Nubian Aquifer being largely recharged prior to and/or during the Last Glacial Maximum (represented by Group I), possibly through the intensification of paleowesterlies; and (2) continued sporadic recharge during the relatively dry and warmer interglacial period (represented by Group II) under conditions similar to those of the present.

Introduction

The Nubian Sandstone Aquifer System (NSAS) is one of the largest fresh groundwater reserves in the world (area: 2×10^6 km^2; volume: 780×10^3 km^3) (Thorweihe, 1990). This transboundary aquifer is present throughout a large area of North Africa, including northwestern Sudan, northeastern Chad, eastern Libya, and western Egypt (inset Fig. 1a). The Nubian Sandstone extends in the Sinai Peninsula; it is exposed at the foothills of the Precambrian basement outcrops in Sinai and in the Negev desert and underlies large segments of the central Sinai Peninsula and the southern part of the Negev desert (Said, 1962; Issar et al., 1972) (Fig. 1). The NSAS is composed of thick (up to 3 km in basin center) sequences of unfossiliferous continental sandstone with intercalated shale of shallow marine and deltaic origin, unconformably overlying basement rocks (Himida, 1970; Shata, 1982; Hesse et al., 1987).

There is a general consensus that the paleoclimatic regimes of the North African Sahara Desert alternated between dry and wet periods throughout the Pleistocene Epoch and that it was during these wet periods that the NSAS was recharged. However, the nature of these wet periods remains a subject of debate. Two main hypotheses have been advocated to address the origin of the fossil water of the NSAS: (1) intensification of paleowesterlies during glacial periods (Sonntag et al., 1978; Sultan et al., 1997; Frumkin et al., 2000; Bartov et al., 2002; Brookes, 2003; Issar, 2003; Issar and Zohar, 2004; Sturchio et al., 2004; Vaks et al., 2006; Issar, 2010; Abouelmagd et al., 2012) or (2) intensification of paleomonsoons during interglacial periods (Yan and Petit-Maire, 1994; Bar-Yosef and Meadow, 1995; Bar-Matthews et al., 2003; Almogi-Labin et al., 2004; Osmond and Dabous, 2004). The model pertaining to intensification of paleowesterlies during the glacial periods is supported by a variety of field, geochronologic, and isotopic evidence. For example, glacial periods were humid in the eastern Mediterranean, as indicated by (1) the isotopic compositions of speleothems collected from a cave in Jerusalem (Frumkin et al., 2000) and from a cave in the central mountain range in Israel (Vaks et al., 2003); (2) the areal extent of deposits from Lake Lisan (precursor of the Dead Sea), which reached its maximum level during the Last Glacial Maximum (Bartov et al., 2002, 2003; Torfstein et al., 2013) or just prior to it (Lisker et al., 2009); and (3) identification of modern westerly wind regimes that produce precipitation that has isotopic compositions similar to those of the NSAS paleowaters (Abouelmagd et al., 2012). The monsoonal hypothesis, in contrast, is supported by a number of arguments including the age record of sapropels over the past 250 ka (Rossignol-Strick, 1983). The organic-rich black layers that were

* Corresponding author at: Department of Geosciences, Western Michigan University, 1903 W. Michigan Avenue, Kalamazoo, Michigan 49008, USA. Fax: +1 269 387 5513.
E-mail address: mohamed.sultan@wmich.edu (M. Sultan).

0033-5894/$ – see front matter © 2013 University of Washington. Published by Elsevier Inc. All rights reserved.
http://dx.doi.org/10.1016/j.yqres.2013.10.017

deposited by the River Nile during heavy African monsoons in the eastern Mediterranean were found to coincide in their depositional age with the astronomically driven maximum summer insolation in the northern tropics. Simulations (from general circulation models) also revealed contemporaneous intensification of African monsoons with increasing summer insolation in the Northern Hemisphere (Prell and Kutzbach, 1987).

There is also a general consensus that the NSAS was largely recharged in previous wet climatic periods. However, geochemical data (O, H stable isotope compositions) for groundwater samples from recharge areas in southern Sinai (Fig. 2), geophysical (electrical resistivity soundings) data, and rainfall – runoff modeling have shown that in some areas where relatively high precipitation occurs, as is the case in Sinai, local recharge areas are still receiving modern recharge (Sultan et al., 2011).

In this study, we investigate the nature of the wet climatic periods that recharged the NSAS and examine whether the NSAS was recharging during relatively dry climatic conditions similar to the ones currently prevailing. Our approach involves (1) estimation of ^{14}C model ages of Nubian paleowaters to identify the timing of paleo-recharge periods; (2) estimation of recharge temperatures for paleowaters from dissolved noble gas concentrations and through comparisons to current mean annual air temperature (MAAT) to examine the nature of recharge periods (low temperatures are indicative of recharge during glacial periods, whereas high temperatures are consistent with recharge during interglacial periods); and (3) examination of the tritium activities in the groundwater from the NSAS and comparison of stable isotopic composition with that of modern precipitation in the region to evaluate the extent of additional modern recharge. The Sinai Peninsula in Egypt was selected as our study area for the reasons discussed below.

Study area

Two main groups of rock units are exposed across the Sinai Peninsula (Fig. 1): (1) the Precambrian basement complex consisting of gneisses, volcano-sedimentary successions, and granitoids of the Arabian–Nubian Shield Massif in the south; and (2) the Phanerozoic sedimentary successions to the north (Sultan et al., 1988; Stern and Kroner, 1993; Blasband et al., 2000). The Phanerozoic successions vary in thickness and composition from south to north. Continental facies (up to 2000 m thick) are dominant in the south, and thick marine facies (~8000 m thick) are dominant in the north (Alsharhan and Salah, 1996). From south to north, gently inclined sedimentary rocks of Paleozoic to Eocene age in central Sinai give way to strongly folded Triassic to Cretaceous Formations that are overlain by Paleocene and Eocene formations. These Precambrian rocks and Phanerozoic sequences are covered by dune fields of Quaternary age in northern Sinai (JICA, 1999).

The NSAS is composed of unfossiliferous continental sandstone of Lower Cretaceous age intercalated with shale of shallow marine and deltaic origin of the Malha Formation in central and southern Sinai (Abdallah et al., 1963) and marine limestone of the Risan Aneiza Formation in northern Sinai (Said, 1971). The Malha and the Risan Aneiza Formations are part of the Nubian Sandstone group that rests unconformably on the basement rock units (Shata, 1982) and is overlain by calcareous sequences of Cenomanian to Upper Eocene age (Said, 1962) (Fig. 1b).

The Sinai Peninsula (61×10^3 km^2) receives relatively high amounts of precipitation compared to the other Egyptian desert areas. Using 3-hourly precipitation data (1998 to 2011) from the Tropical Rainfall Measuring Mission (TRMM; v7A), the average annual precipitation over the Western Desert, Eastern Desert, and Sinai was found to be 9 mm/yr, 13 mm/yr, and 70 mm/yr, respectively. TRMM is a joint space mission between NASA and the Japan Aerospace Exploration Agency (JAXA) that was designed to monitor tropical and subtropical rainfall. The mountainous basement complex in southern Sinai receives the highest amounts of precipitation in Sinai (EMA, 1996; Geb, 2000); precipitation is collected and channeled through main streams by the extensive stream network in the area. The main streams at the foothills and north of the basement complex are floored by the NSAS outcrop, which provides opportunities for infiltration and recharge through initial and transmission losses (Fig. 1). Rainfall in the area is caused primarily by cyclonic winter storms passing over the Mediterranean depressions and tracking southeast. Because of their sporadic nature and the presence of extensive stream networks that channel runoff from large watersheds into a few main valleys, these storms are often associated with flash-flooding events.

Analytical methods

Fieldwork was conducted in January and June of 2010 to sample groundwater from 12 drilled wells and from the Ayun Musa spring, which taps the NSAS and from three open wells in the fractured basement. The wells are evenly distributed over the northern, central, and southern parts of the Sinai Peninsula and along the Gulf of Suez coastal zone (Fig. 1). The samples from the NSAS define two groups on the basis of total well depth (TD), depth to static water level (DWL), and proximity to recharge areas. Group I samples were collected from eight deep wells (TD: 747–1250 m; DWL: 137–377 m) and from a spring, all of which are located far (>150 km) from recharge areas (Fig. 1). These include Arif El Naqa 2, El Themed 2, El Hasana 3, Sudr El Hetan 3, El Kuntella 3, Nekhel 5, Egirah El Far 4, El Berouk 4, and Ayun Musa. Group II samples (El Rueikna 3, Mekatab 3, Nadya El Soda, and Regwa 12) were collected from four shallow wells (TD: 63–366 m; DWL: 19–56 m) that are proximal (<40 km) to recharge areas (Fig. 1). Three additional samples were collected from wells (Haroun, Halwagy, and Dir El Banat) tapping alluvial and fractured basement aquifers in southern Sinai. Samples were collected to be analyzed for (1) stable isotopic compositions of hydrogen and oxygen in water and carbon in dissolved inorganic carbon (DIC); (2) ^{14}C abundance in DIC for model age estimation; (3) dissolved noble gas concentrations for estimation of noble gas recharge temperatures; and (4) tritium (^3H) activities. The analytical methods used for each of these analyses are briefly described below.

Wells were pumped for a minimum of 30 min prior to sample collection. The wells were purged until the pH and Ec readings stabilized and the sampled groundwater was clear. Unfiltered and unacidified water samples were collected in tightly capped 30-mL glass bottles for stable isotopic (δ^2H, $\delta^{18}O$, and $\delta^{13}C$) analyses (Tables 1 and 2). The H and O isotopic ratios were analyzed using a Picarro Cavity Ring-down Spectroscopy (CRDS) laser system (Lehmann et al., 2009). Carbon isotope analysis of DIC was performed on CO_2 released by acid digestion using H_3PO_4 and measured by dual-inlet isotope-ratio mass spectrometry. Hydrogen, oxygen, and carbon stable isotope ratios are reported using conventional delta (δ) notation, in units of per mil (‰) deviation relative to the Vienna Standard Mean Ocean Water (V-SMOW) whereby

$$\delta, ‰ = \left[\left(R_{sample} - R_{std}\right)/R_{std}\right] \times 1000$$

and $R = {}^2H/{}^1H$, ${}^{18}O/{}^{16}O$ or ${}^{13}C/{}^{12}C$ (Coplen, 1996). Reproducibility of δ values for ^2H is ± 1‰ and those of ^{18}O and ^{13}C are ±0.2‰ and ± 0.1‰, respectively.

Tritium (^3H), the radioactive isotope of hydrogen, was produced during the atmospheric testing of nuclear fusion bombs between 1953 and 1964 and is used as a tracer for recharge, flow, and mixing processes of young groundwater (Plummer et al., 1993). Because natural background tritium activity in the atmosphere was low (about 5 TU) prior to bomb testing, groundwater with tritium activities less than about 0.5 TU must have been derived from precipitation that fell before 1953. Tritium activity was determined by counting after tritium enrichment by electrolysis of the water. A half-life of 12.43 yr was used to calculate the resulting TU (tritium unit) values, where 1 TU is equal to a tritium/hydrogen ratio of 10^{-18}. Analyses (O, H, ^3H) were conducted at Isotech Laboratories, in Champaign, Illinois.

https://doi.org/10.1016/j.yqres.2013.10.017 Published online by Cambridge University Press

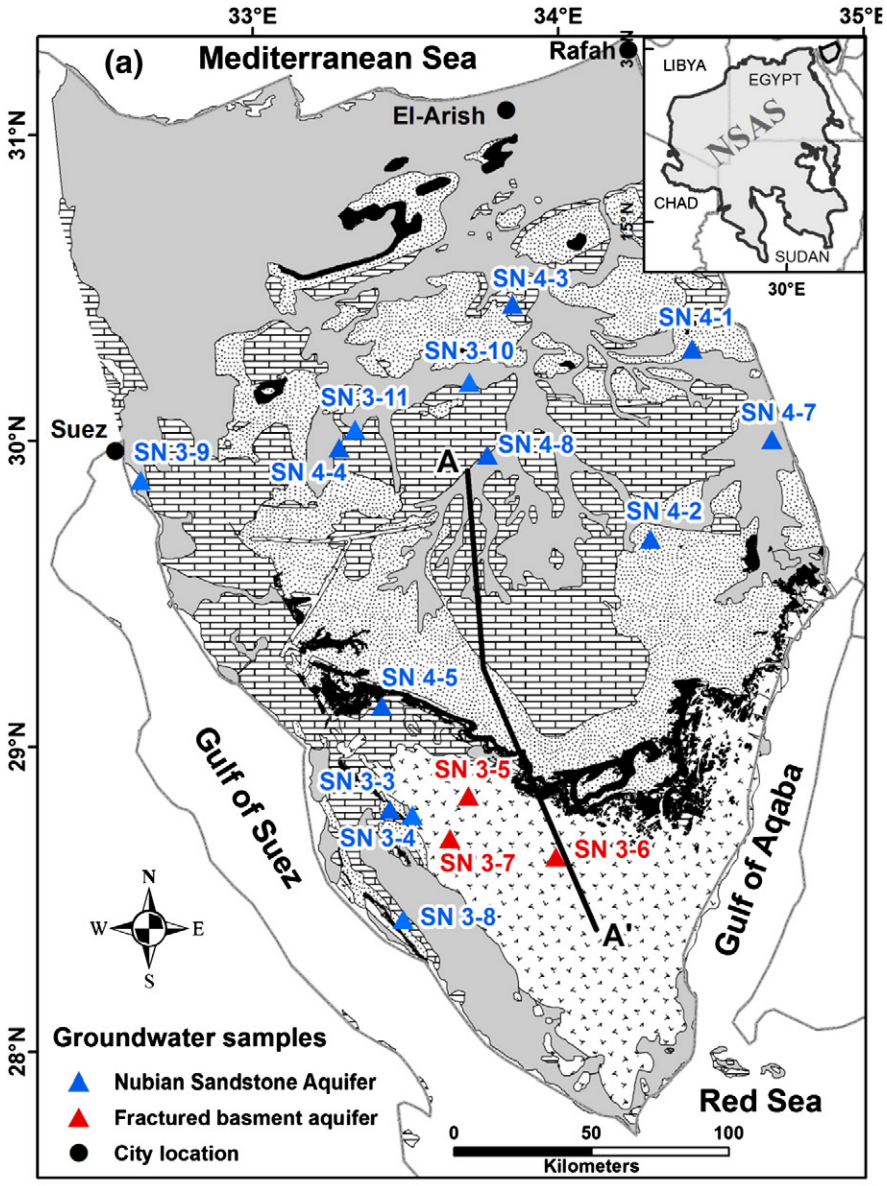

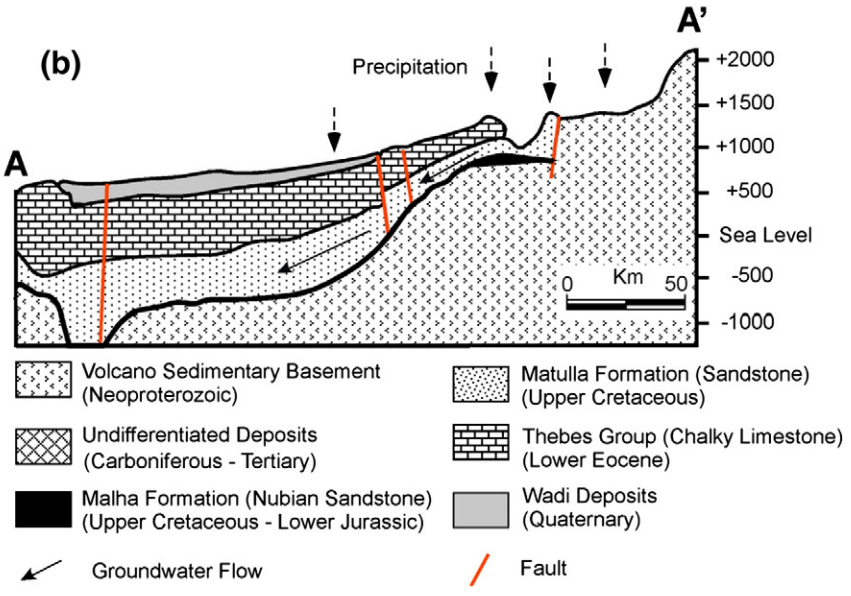

https://doi.org/10.1016/j.yqres.2013.10.017 Published online by Cambridge University Press

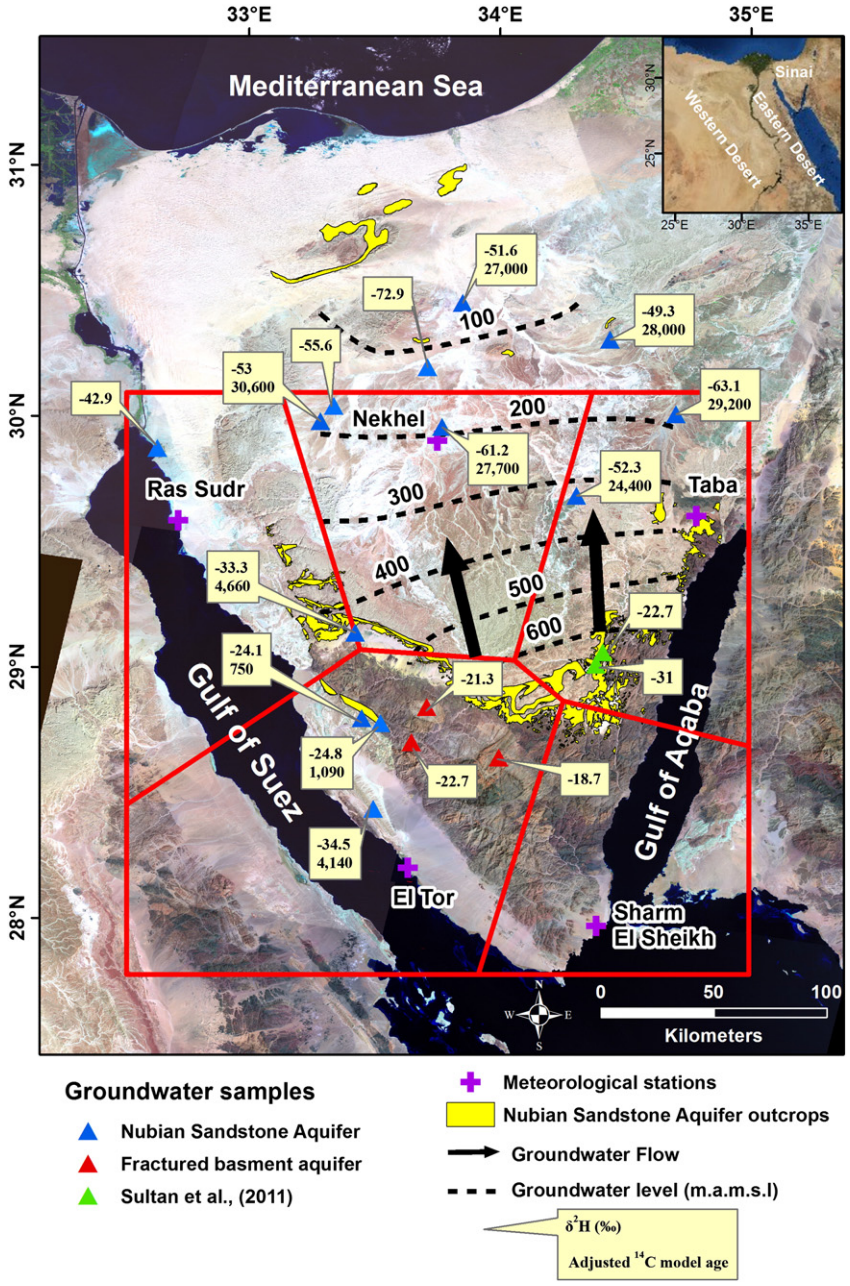

Figure 2. A base map false-color Landsat TM image (USGS, 2003) showing (1) our groundwater sample locations from wells and a spring tapping the NSAS (blue triangles) and from wells tapping the fractured basement aquifer (red triangles); (2) groundwater sample locations for open wells tapping the NSAS in the recharge areas (green triangles) (Sultan et al., 2011); (3) groundwater levels (dashed lines) and flow directions (black arrows); and (4) δ^2H value (yellow box: upper), adjusted ^{14}C model age (yellow box: lower). Also shown is a graphical representation for polygons (outlined by red lines) defined by the Thiessen method that was applied to interpolate present-day mean weighted annual temperature from meteorological stations (purple cross) to the surrounding areas including the Nubian Sandstone Aquifer outcrops.

Unfiltered water samples were collected in tightly capped 250-mL glass bottles for ^{14}C analysis using the accelerator mass spectrometry (AMS) technique. The DIC was extracted in vacuum by acidifying the water sample. The extracted CO_2 was cryogenically purified from the other reaction products and catalytically converted to graphite using the method of Vogel et al. (1984). Graphite $^{14}C/^{13}C$ ratios were measured using a 0.5-MeV accelerator mass spectrometer. The sample ratios were compared to the ratio measured for the oxalic acid standard reference material (NBS SRM 4990). The ^{14}C data are reported both in terms of percent modern carbon and in terms of conventional radiocarbon ages (Stuiver and Polach, 1977) reported in ^{14}C years before 1950 (^{14}C yr BP); a ^{14}C half-life of 5568 yr was used, and correction for isotopic fractionation was applied (Cherkinsky et al., 2010). The analytical precision of the AMS ^{14}C results is $\pm$0.9%. Analyses were performed at the University of Georgia's Center for Applied Isotope Studies (CAIS) and by Beta Analytic in Miami, Florida. To account for the carbonate

Figure 1. (a) Location map showing the locations of our groundwater samples that were collected from 12 drilled wells and from a spring tapping the NSAS (blue triangles) and from three open wells tapping the fractured basement aquifer (red triangles). Also shown are the distribution of Neoproterozoic outcrops, overlying Phanerozoic rock units, and the recharge areas of the NSAS (Upper Jurassic to Lower Cretaceous Malha Formation outcrops). (b) N–S trending cross section along line A–A′ plotted on Fig. 1b modified from Gheith and Sultan (2002).

https://doi.org/10.1016/j.yqres.2013.10.017 Published online by Cambridge University Press

Table 1
Sample locations, well information, O and H isotopic compositions, and tritium activities for groundwater samples from wells tapping the NSAS and the fractured basement in Sinai.

ID	Name	Latitude	Longitude	Aquifer/	TD[a]	DWL[a]	TDS[b]	δ^2H[c]	$\delta^{18}O$[c]	^3H[c]	Group
		N	E	Well	(m)	(m)	(mg/L)	(‰)	(‰)	TU	
SN4-1	Arif El Naqa 2	30°18.21′	34°26.30′	NSS/D	870	271	3810	−49.3	−7.62	–	I
SN4-2	El Themed 2	29°40.80′	34°18.20′	NSS/D	747	376.8	1830	−52.3	−7.7	–	I
SN4-3	El Hasana 3	30°26.99′	33°51.06′	NSS/D	1200	200	3260	−51.6	−7.19	–	I
SN4-4	Sudr El Hetan 3	29°58.70′	33°16.95′	NSS/D	1040	270	1740	−53	−7.85	–	I
SN4-5	El Rueikna 3	29°08.06′	33°25.35′	NSS/D	–	55.6	480	−33.3	−5.89	–	II
SN4-7	El Kuntella 3	30°00.38′	34°42.04′	NSS/D	1121	353.4	1827	−63.1	−8.85	–	I
SN4-8	Nekhel 5	29°57.27′	33°46.08′	NSS/D	1200	200.6	1622	−61.2	−8.81	–	I
SN3-3	Mekatab 3	28°47.71′	33°26.89′	NSS/D	366	49.7	953	−24.1	−4.84	<1.0	II
SN3-4	Nadya El Soda	28°46.55′	33°31.35′	NSS/D	63	–	934	−24.8	−4.93	2.78 ± 0.29	II
SN3-5	Haroun	28°50.37′	33°42.41′	FB/O	31	29.7	827	−21.3	−4.13	2.42 ± 0.27	II
SN3-6	Halwagy	28°38.33′	33°59.62′	FB/O	–	30	868	−18.7	−3.36	2.55 ± 0.30	II
SN3-7	Dir El Banat	28°42.00′	33°38.80′	FB/O	–	–	675	−22.7	−4.54	3.04 ± 0.28	II
SN3-8	Regwa 12	28°26.05′	33°29.59′	NSS/D	–	18.4	622	−34.5	−5.72	<1.0	II
SN3-9	Ayun Musa	29°52.28′	32°38.03′	NSS/S	n/a	n/a	2778	−42.9	−6.53	<1.0	I
SN3-10	El Berouk 4	30°11.60′	33°42.58′	NSS/D	955	137	2682	−72.9	−9.59	<1.0	I
SN3-11	Erirah El Far 4	30°02.35′	33°20.15′	NSS/D	1250	–	2215	−55.6	−8	<1.0	I

Abbreviations: NSS: Nubian Sandstone; FB: fractured basement; D: drilled well; O: open well; S: spring; TU: tritium unit.
[a] Data collected from field work and from JICA (1999).
[b] Western Michigan University geochemical labs.
[c] Analyzed at Isotech Laboratories, Champaign, Illinois.

reactions that occur in groundwater systems, traditional ^{14}C age adjustment approaches (Vogel, 1967; Tamers, 1975) based on single water analyses were applied by using the NetpathXL computer code (Parkhurst and Charlton, 2008), which is a revised version of NETPATH (Plummer et al., 1994). The adjusted ^{14}C model ages and their average values are reported for each of the measured samples in Table 2, with units of "yr BP.".

Samples were collected from seven wells and analyzed for their noble gas concentrations using procedures described in Weiss (1968) and Stute et al. (1995) (Table 3). The following measures were taken to avoid exchange with atmospheric air and/or partial degassing: (1) predesigned polyvinyl chloride (PVC) tube was attached to the borehole outlet with a flexible coupling; (2) well water was allowed to flow through a transparent plastic hose to allow inspection for the presence of air bubbles, and then it was allowed to flow into a copper tube (diameter: ~1 cm; length: 53 cm; volume: ~22 cm^3) for several minutes before the copper tube was sealed with stainless steel clamps; and (3) a regulator valve was placed at one end of the copper tube to increase the pressure in order to minimize air bubble formation.

Dissolved gases were extracted from the copper tubes on a vacuum line. The water was transferred from the copper tube into a large stainless steel flask under a high-vacuum, closed system. The flask was then heated while a smaller flask was chilled, creating a flux of gas from the large flask into the small flask. The small flask was then sealed before being transferred to the mass spectrometry line. The individual noble gases were separated and analyzed using a quadrupole mass spectrometer; they are presented as concentrations (cm^3 STP g^{-1}) in Table 3. The reproducibility of the measurements was ± 2% for Ne, ± 3% for Ar, and ± 5% for both Kr and Xe. The noble gas measurements were performed at the University of Utah's Dissolved and Noble Gas Laboratory, in Salt Lake City, Utah.

Noble gas recharge temperatures (NGTs) were calculated (Table 3) using measured concentrations of Ne, Ar, Kr, and Xe and applying methods described by Solomon et al. (1998) and Manning and Solomon (2003). The adopted algorithm accounts for the effects of salinity and elevation on the solubility of atmosphere-derived noble gases. Noble gas solubility decreases with increasing salinity (Mazor, 1972; Pinti and Van Drom, 1988) and increases with increasing

Table 2
Carbon isotopic data and ^{14}C model ages for investigated groundwater samples.

ID	Name	$\delta^{13}C$	Unadjusted age		Adjusted age		
			% modern C	^{14}C yr BP[c]	^{14}C model ages (yr BP)		
		(‰)	(pmC)	(^{14}C yr BP)	Vogel (1967)	Tamers (1975)	Average
SN4-1[a]	Arif El Naqa 2	−5.5	2.42 ± 0.03	29,900	29,400	26,600	28,000
SN4-2[a]	El Themed 2	−7.2	3.90 ± 0.03	26,100	25,500	23,300	24,400
SN4-3[a]	El Hasana 3	−6.1	2.70 ± 0.03	29,000	28,500	25,500	27,000
SN4-4[a]	Sudr El Hetan 3	−9.1	1.82 ± 0.02	32,200	31,800	29,400	30,600
SN4-5[a]	El Rueikna 3	−7.3	46.3 ± 0.2	6180	5020	4290	4660
SN4-7[a]	El Kuntella 3	−6.6	2.03 ± 0.02	31,300	30,900	27,500	29,200
SN4-8[a]	Nekhel 5	−7.6	2.49 ± 0.03	29,700	29,200	26,100	27,700
SN3-3[b]	Mekatab 3	−12.8	80.5 ± 0.4	1740	450	1050	750
SN 3-4[b]	Nadya El Soda	−13.4	84.5 ± 0.4	1350	–	1090	1090
SN 3-8[b]	Regwa 12	−14.1	51.9 ± 0.3	5260	4080	4200	4140
SN 3-9[b]	Ayun Musa	−11.4	–	–	–	–	–
SN 3-10[b]	El Berouk 4	−17.7	–	–	–	–	–
SN 3-11[b]	Erirah El Far 4	−11.8	–	–	–	–	–

[a] Analyzed at the Center for Applied Isotopic Studies (CAIS), University of Georgia, Athens, Georgia.
[b] Analyzed at Beta Analytic, Miami, Florida.
[c] Uncorrected ^{14}C age (Stuiver and Polach, 1977).

https://doi.org/10.1016/j.yqres.2013.10.017 Published online by Cambridge University Press

Table 3
Noble gas concentration data for investigated groundwater samples and estimated recharge temperatures.

ID	Concentrations (cm^3 STP g^{-1})							Temp[a] (°C)	NGT[b] (°C)
	Name	He [10^{-7}]	Ne [10^{-7}]	Ar [10^{-4}]	Kr [10^{-8}]	Xe [10^{-8}]	R/Ra		
SN4-1	Arif El Naqa 2	5.71	2.49	3.23	6.57	0.88	0.12	33.6	20.6 ± 0.4
SN4-2	El Themed 2	7.49	7.15	5.50	10.2	1.10	0.25	30.5	21.1 ± 1.6
SN4-3	El Hasana 3	9.14	2.11	3.13	7.58	0.94	0.08	39.1	17.5 ± 1.3
SN4-5	El Rueikna 3	1.01	2.03	2.97	6.77	0.87	0.56	27.2	20.6 ± 0.7
SN3-3	Mekatab 3	1.82	2.03	2.72	6.04	0.74	0.36	29.5	26.2 ± 0.9
SN4-7	El Kuntella 3	533	22.9	15.6	23.1	2.15	0.09	33.6	18.1 ± 2.5
SN4-8	Nekhel 5	22.9	6.09	5.90	11.8	1.15	0.10	38.6	22.0 ± 3.8

[a] Groundwater temperature.
[b] Noble gas recharge temperature calculated (RT-Calculator; version 1) from the measured noble gas concentration using methods described by Solomon et al. (1998) and Manning and Solomon (2003).

atmospheric pressure. The total dissolved solids (TDS) concentrations in our samples range from 480 to 3800 mg/L (Table 1), and the average elevation of the recharge area in south-central Sinai was estimated from a digital elevation model (DEM) to be 761 m above mean sea level (amsl).

Findings and discussion

Examination of the groundwater head data from the sampled wells reveals a general northward groundwater flow direction for the NSAS from the recharge area in the south (Fig. 2, black arrow). The groundwater head (Table 1) shows a decrease from over 600 m amsl in the recharge area in the south (El Rueikna 3 well) to less than 100 m amsl in the north (El Hasana 3 well). Similar findings were reported by Issar et al. (1972), who reported a general groundwater flow in the NSAS from the Nubian outcrops at the foothills of the basement in southern Sinai toward the Mediterranean Sea, the Gulf of Aqaba, and the Gulf of Suez. We were unable to verify the inferred flow directions to the northeast and to the northwest (Issar et al., 1972) given the limited availability of head data for the eastern and western regions of Sinai.

We examined the stable isotope compositions, ^{14}C model ages, and noble gas recharge temperatures of the investigated samples in view of the inferred groundwater flow direction; samples within both Group I and Group II have similar isotopic compositions, model ages, and NGTs, yet the two groups were found to be dissimilar. These data were used to gain insights into the timing of groundwater recharge for Groups I and II samples and to infer the prevailing climatic conditions at the times of recharge.

Stable isotope ratios

The stable isotope ratios of H and O for the investigated samples are given in Table 1 and are shown in Figure 3, which also includes data from the present study in comparison with (1) groundwater samples collected from fractured basement aquifers in the southern Sinai Peninsula, and (2) average isotopic compositions of modern rainfall collected from Rafah and El Arish meteorological stations (IAEA and WISER, 2010). Examination of Table 1 and Figure 3 shows that the δ^2H and $\delta^{18}O$ values of Group I samples are depleted ($\delta^{18}O$: −9.59 to −6.53‰; δ^2H: −72.9 to −42.9‰) compared to Group II samples ($\delta^{18}O$: −5.89 to −4.84‰; δ^2H: −34.5 to −24.1‰) and those collected from fractured basement ($\delta^{18}O$: −4.54 to −3.36‰; δ^2H: −22.7 to −18.7‰). Most of the Group I samples fall on or near the global meteoric water line (GMWL), $\delta^2H = 8\,\delta^{18}O + 10$ (Craig, 1961), whereas samples from Group II, the meteorological stations (Rafah and El Arish), and from the fractured basement aquifer fall between the GMWL and the east Mediterranean meteoric water line (MMWL; $\delta^2H = 8$

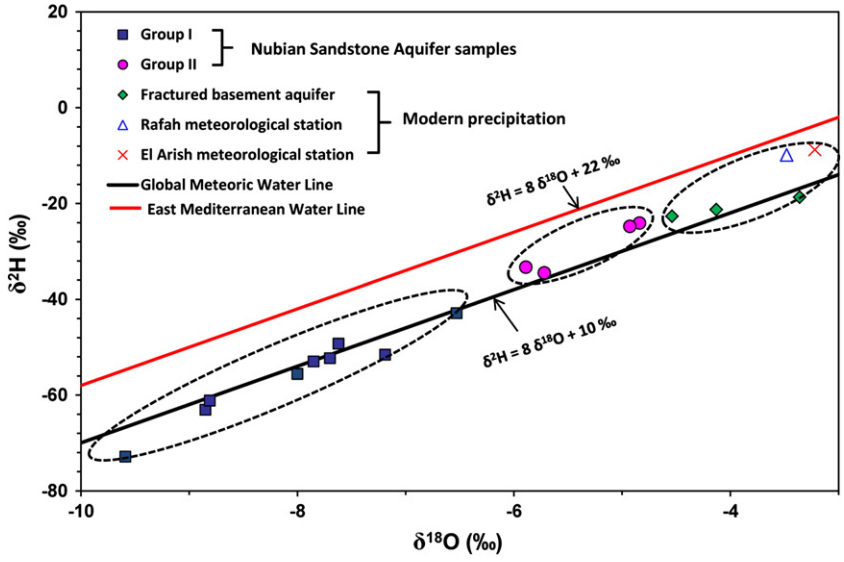

Figure 3. δ^2H vs. $\delta^{18}O$ plot for (1) depleted groundwater samples collected from Nubian Sandstone Aquifer of Sinai Peninsula classified as Group I; (2) enriched groundwater samples collected from Nubian Sandstone Aquifer of Sinai Peninsula classified as Group II; (3) composition of modern rainfall from Rafah and El Arish meteorological stations (IAEA and WISER, 2010); and (4) composition of groundwater samples from the fractured basement aquifer. Also shown is the Global Meteoric Water Line ($\delta D = 8\,\delta^{18}O + 10$) of Craig (1961) and the East Mediterranean Water Line of Gat et al. (1969).

https://doi.org/10.1016/j.yqres.2013.10.017 Published online by Cambridge University Press

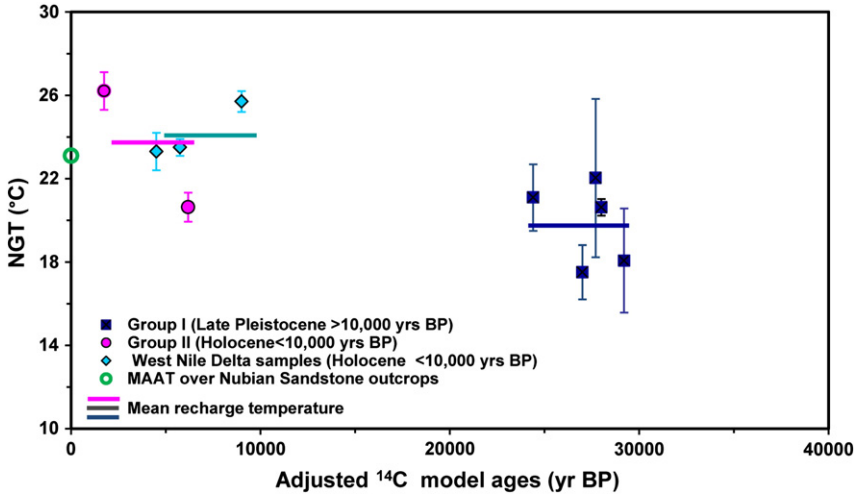

Figure 4. Calculated noble gas recharge temperatures vs. adjusted ^{14}C model ages for Group I Pleistocene samples, Group II Holocene samples, and three Holocene groundwater samples collected from Western Nile Delta (Aeschbach-Hertig, 2006; Aeschbach-Hertig et al., 2006a, 2006b, 2007).

$\delta^{18}O + 22$) (Gat et al., 1969) indicating differences in precipitation moisture sources.

The basement samples are believed to represent modern meteoric precipitation, and they have isotopic compositions similar to those of average rainfall compositions over the Rafah ($\delta^{18}O$: −3.48‰; $\delta^{2}H$: −9.86‰) and El Arish ($\delta^{18}O$: −3.22‰; $\delta^{2}H$: −8.81‰) meteorological stations (Fig. 1). The depleted nature of the Group I samples and the enriched nature of the Group II samples are consistent with the former being recharged mainly under conditions cooler than those of the present day (Gat et al., 1969) and the latter being recharged primarily during warmer periods, similar to the present. The wide range of isotopic compositions for Group I samples and the fact that a few have compositions that approach those of Group II could be interpreted to indicate mixing of older Group I waters with younger Group II waters.

Radiocarbon model ages

The calculation of accurate groundwater age from ^{14}C measurements can be complicated by the effects of carbonate rock–water interactions, groundwater mixing, and diffusive exchange of ^{14}C with aquitards (Fontes and Garnier, 1979; Sanford, 1997). Depending on aquifer-specific considerations, these processes can affect apparent groundwater ages substantially, such that all ^{14}C groundwater ages are highly model-dependent (e.g., Plummer and Sprinkle, 2001). Fortunately, the effects of carbonate rock–water interaction and diffusive exchange with aquitards are relatively minimal in thick sandstone aquifers. We report conventional ^{14}C ages that are uncorrected for these effects, along with adjusted ^{14}C model ages calculated by NetPath XL (Parkhurst and Charlton, 2008) using the adjustments proposed by Vogel (1967) and Tamers (1975). The reasonable agreement between the calculated ^{14}C model ages indicates to us that they are reliable indicators of mean subsurface residence time, albeit with significant errors. Nonetheless, adjusted ^{14}C model ages (Table 2, Figs. 2 and 4) show distinct ranges for Groups I and II. Group I samples are older and originated from precipitation during the late Pleistocene (adjusted ^{14}C model ages: ~24,000 yr BP to ~31,000 yr BP), which we infer to have been a period of wet climate, whereas Group II samples are younger and were formed from precipitation during the Holocene (adjusted ^{14}C model ages: ~700 yr BP to ~4700 yr BP). The adjusted ^{14}C model ages of the Group I samples should be further corrected by adding 3000 to 4000 yr to account for the offset of the ^{14}C time scale determined from calibration of the ^{14}C time scale with precise comparison of mass spectrometric measurements of ^{14}C and ^{230}Th–^{234}U–^{238}U systematics of pristine corals (Fairbanks et al., 2005). This correction yields a corresponding model age range of 27,000–35,000 yr BP; this range slightly pre-dates the 19,000–26,500 yr BP Last Glacial Maximum (Clark et al., 2009) and it overlaps the 31–35 ka high stand of Lake Lisan (Pleistocene precursor of the Dead Sea) according to U–Th dates on cave stromatolites (Lisker et al., 2009). However, we cannot be certain that potential reactions with carbonate rocks and diffusive effects have not increased the apparent ^{14}C ages in our Group I water samples. The younger ages of our Group II water samples support the interpretation that the NSAS has also received recharge contributions during the Holocene Period.

Table 4
Calculation of the modern average weighted temperatures over Nubian Sandstone recharge areas in central Sinai Peninsula using the Thiessen polygon method.

Station name	Latitude (DD)	Longitude (DD)	MAAT station[a] (°C)	Recharge area[b] (km^2)	Recharge area[c] (fraction)	MAAT[d] (°C)
Ras Sudr	29.58300	33.71700	20.6	246	0.182	3.76
Nekhel	29.68000	34.30333	17.8	47	0.352	0.63
Taba	30.44983	33.85100	25	695	0.516	12.9
El Tor	29.97833	33.28250	21.7	216	0.161	3.48
Sharm El Sheikh	29.13433	33.42250	21.7	143	0.107	2.31
TOTAL				1347	0.100	23.1

[a] Average temperature recorded over the past 35 yr (NCDC, 2012).
[b] Area of Nubian outcrops (recharge areas) that were assigned to each of the five meteorological stations using the Thiessen polygon method.
[c] Proportion of Nubian outcrops that were assigned to each of the five stations.
[d] MAAT for recharge area (23.1°C) calculated from the product of the MAAT for each station and the proportion of recharge areas affected by the individual stations.

Tritium activities

Tritium activities for the groundwater samples collected from fractured basement ranged from 2.4 ± 0.3 to 3.0 ± 0.3 TU, indicating that all waters were derived at least partly from precipitation that occurred within the past 60 yr. None of the analyzed Group I samples had detectable tritium activities (<1 TU), whereas one of the Group II samples (Nadya El Soda) had tritium activity (2.8 ± 0.3) indicative of the presence of post-bomb precipitation (younger than ~60 yr; Table 1). This sample also had slightly less ^{14}C activity than modern water (84.5% modern C), indicating possible mixing of older and younger water in this well, which is located in a wide wadi near the basement-Nubian Sandstone contact. Alternatively, it may reflect the characteristic ^{14}C activity of recharge water in this region (Fontes and

https://doi.org/10.1016/j.yqres.2013.10.017 Published online by Cambridge University Press

Garnier, 1979). Modern precipitation over the Nubian Aquifer outcrops can introduce post-bomb tritium activities into the NSAS during sporadic flash flood events; these events yield voluminous recharge that accumulates in coarse sediments of the alluvial channels and in the fractured rock flooring these channels. Measurable tritium may occur in areas proximal to recharge zones, but is not likely to be found in distant areas.

Noble gas paleothermometry

The dissolved noble gas (He, Ne, Ar, Kr, and Xe) concentrations in groundwater have been used successfully in many paleoclimatic studies in conjunction with ^{14}C model ages to determine recharge temperatures during the Quaternary Period (Mazor, 1972; Stute and Schlosser, 1993; Kipfer et al., 2002; Klump et al., 2007). Atmospheric noble gases are incorporated into groundwater by exchanges between recharge water and soil air within the unsaturated zone. As the water enters the saturated zone, the gas exchange stops and the noble gas concentrations are retained by the water as a tracer for the environmental conditions prevailing during infiltration. Because noble gases are conservative and inert, the atmospheric noble gas concentrations are preserved in groundwater. Because the solubility of the noble gases significantly depends on the water temperature during gas exchange, especially for Ar, Kr, and Xe (Mazor, 1972), the dissolved noble gases in groundwater can potentially be used to extract recharge temperature.

The NGTs derived for the Group I samples range from 17.5° ± 1.3°C (El Hasana 3) to 22.0° ± 3.8°C (Nekhel 5) and average 19.9°C; NGTs for Group II samples are 20.6° ± 0.7°C (El Rueikna 3) and 26.2° ± 0.9°C (Mekatab 3), and their average is 23.9°C (Table 3). Figure 4 shows the NGTs plotted versus adjusted ^{14}C model ages for Group I samples (late Pleistocene waters, >10 ka BP), Group II samples (Holocene waters <10 ka BP), and three Holocene (4.5–9 ka BP) groundwater samples collected from the Tertiary-Upper Cretaceous water-bearing formations that underlie the southwestern Nile Delta in Egypt (Aeschbach-Hertig, 2006; Aeschbach-Hertig et al., 2006a, 2006b, 2007). Also shown is the average mean annual air temperature (MAAT) over the recharge area.

The average NGT for our Group I Pleistocene samples is similar to the average NGT (20°C) reported for five Nubian groundwater samples from the Western Desert (Patterson, 2003). Our results from the Sinai NSAS are consistent with reported findings from fossil groundwater aquifers in North Africa. Throughout a major recharge period that occurred 45 to 23 ka, the NGTs for the Continental Intercalaire aquifer within the Northwestern Sahara Aquifer System (in Algeria, Tunisia, and Libya) are estimated to have been 2–3°C lower than the MAAT (Guendouz et al., 1998). The Iullemeden Aquifer System (in Mali, Niger, and Nigeria) was recharged between 28 ka and 23.2 ka, during which time the NGTs were at least 5–6°C lower than MAAT (Edmunds et al., 1999). The groundwater ages cited above correspond to glacial periods identified from North Atlantic marine record (Bond et al., 1993), and the extracted recharge temperatures are generally lower than MAAT in the investigated areas by 2–7°C. Such lower temperatures are to be expected if the recharge was from precipitation during cool glacial periods.

Figure 4 shows that the average NGT for Group II samples is 4.0°C higher than that of Group I, is similar to that computed for the Holocene groundwater samples collected from the Western Nile Delta (range: 20.6–26.2°C; average: 23.9°C), and is similar to that of the MAAT (23°C) over the recharge area for the NSAS in southern and central Sinai. The MAAT over the recharge area was estimated by calculating the MAAT over each of the five meteorological stations (Ras Sudr, Nekhel, Taba, Sharm El Sheikh, and El Tor) that are proximal to the recharge areas, interpolating the calculated temperatures to the surrounding areas (red polygons in Fig. 2) using the Thiessen polygon interpolation technique. The MAAT for the entire recharge area was then calculated taking into consideration the proportion of recharge areas affected by conditions at each of the individual five stations. For example, inspection of Figure 2 and Table 4 shows that over 50% of the recharge areas are affected by conditions recorded at the El Tor station. Temperature data was extracted from the National Oceanic and Atmospheric Administration's (NOAA's) National Climatic Data Center database (NCDC, 2012).

We interpret these results to indicate that the NSAS in Sinai was largely recharged during the last glacial period (represented by Group I waters) but is still receiving modest contributions during relatively dry interglacial periods (represented by Group II waters). This interpretation is also supported by the spatial distribution of Group I and II samples. As described earlier, the NSAS recharge takes place where the Nubian outcrops are exposed adjacent to the basement complex in central Sinai; with time, infiltrating water feeding the NSAS flows away from the recharge zone as the aquifer formations dip to the north toward the Mediterranean Sea (Figs. 1b, 2). Given the differences in ages and isotopic compositions between Group I and Group II samples, with Group II samples being younger and more enriched in their isotopic composition, one would expect that the younger and more enriched Holocene Group II samples should be found in areas proximal to recharge areas, and the older and more depleted Group I samples should be distant from these areas. Inspection of Figure 2 shows that indeed this is the case. We speculate that some mixing between Group I and II groundwater types could be occurring along groundwater flow lines.

Summary

Paleoclimatic information for the Sinai Peninsula was gained from the analysis of 16 samples collected from drilled and open wells and from a spring tapping the NSAS and fractured basement aquifers in Sinai. The analyses performed included (1) stable isotopic compositions of H_2O; (2) ^{14}C isotopic abundances and model ages; (3) tritium activities; and (4) recharge temperatures from noble gas concentrations. The samples define two groups on the basis of well depth, depth to static water level, and proximity to recharge areas. Group I samples were collected from deep wells that are distant from recharge areas (>150 km) whereas Group II samples were collected from shallow wells that are proximal to recharge areas.

Group I samples yield adjusted ^{14}C model ages ranging from ~24,000 yr BP to ~31,000 yr BP, depleted isotopic compositions compared to modern precipitation (from meteorological stations and from the fractured basement aquifer), no detectable tritium, and low NGTs compared to mean annual air temperature. The range and the average NGT for our Group I Pleistocene samples are similar to the average recharge temperature reported for Nubian groundwater samples from the Western Desert, and they are consistent with similar findings for other fossil groundwater aquifers in North Africa. The obtained ages, isotopic compositions, and recharge temperatures are all consistent with Group I samples being largely recharged in cold climatic conditions during and/or before the Last Glacial Maximum.

The remaining four samples from the NSAS were assigned to Group II. These samples yielded Holocene ^{14}C model ages and isotopic compositions that are enriched compared to Group I samples but are similar to, or approach the compositions of, modern precipitation. These ^{14}C model ages and isotopic compositions, together with the presence of detectable tritium in one of the Group II samples, support the interpretation that groundwater from this group originated largely from precipitation during the Holocene period. Despite the fact that samples from Group I are similar to one another and distinct from those assigned to Group II, mixing between groundwater assigned to each of these groups could not be ruled out. Additional studies are needed to investigate the extent to which mixing could have occurred.

The extracted NGTs for Group II samples are similar to those reported for three Holocene groundwater samples from the Tertiary–Upper Cretaceous water-bearing formations that underlie the southwestern Nile Delta, in Egypt. Our findings are consistent with recharge of the Group II samples during conditions similar to those of the present.

https://doi.org/10.1016/j.yqres.2013.10.017 Published online by Cambridge University Press

We interpret these results to indicate that the NSAS was largely recharged during the last glacial period (represented by Group I waters) but that it is still receiving modest contributions during the Holocene period (represented by Group II waters). This model is also supported by the spatial distribution of Group I and II samples, where the younger Holocene Group II samples are found in areas proximal to recharge areas, and the older Group II samples are found in areas distant from recharge areas. Our findings suggest that the wet periods in northern Africa were glacial periods; during these periods paleowesterlies were intensified and the Saharan aquifers were recharged. During the interleaving dry periods such as the one prevailing at present, recharge is modest and is localized to areas where the aquifer crops out and where precipitation is relatively high (e.g., southern Sinai in NSAS). Similar studies are recommended to investigate the validity of this hypothesis over the remaining Saharan aquifers.

Acknowledgments

This study is supported by the National Aeronautics and Space Administration (NASA) (grant NNX08AJ85G) and by the North Atlantic Treaty Organization (NATO) Science for Peace (grant SFP 982614) grants to Western Michigan University. We thank the Editor and the Reviewers of Quaternary Research for their instructive comments and suggestions, Professor K. Solomon and Mr. A. Rigby (The University of Utah, Salt Lake City, Utah) for providing the required field training for sampling noble gases, Professor W. Aeschbach-Hertig (University of Heidelberg) for the constructive discussion about the paleotemperatures of the southwestern Nile Delta region.

References

Abdallah, A.M., Adindani, A., Fahmy, N., 1963. Stratigraphy of Upper Paleozoic Rocks, Western Side of the Gulf of Suez, Egypt. Egyptian Geological Survey 1–18.

Abouelmagd, A., Sultan, M., Milewski, A., Kehew, A.E., Sturchio, N.C., Soliman, F., Krishnamurthy, R.V., Cutrim, E., 2012. Toward a better understanding of palaeoclimatic regimes that recharged the fossil aquifers in North Africa: inferences from stable isotope and remote sensing data. Palaeogeography, Palaeoclimatology, Palaeoecology 329–330, 137–149.

Aeschbach-Hertig, W., 2006. Environmental tracer study of groundwater recharge near the Nile Delta, Egypt. DPG-Tagung, Heidelberg, unpublished report.

Aeschbach-Hertig, W., El-Gamal, H., Dahab, K., Kipfer, R., Bonani, G., 2006a. Environmental tracer study of groundwater recharge near the Nile Delta, Egypt. Determining paleotemperature and other variables by using an error-weighted, nonlinear inversion of noble gas concentrations in water. Geochimica et Cosmochimica Acta 63, 2315–2336.

Aeschbach-Hertig, W., El-Gamal, H., Dahab, K., Kipfer, R., Hajdas, I., Bonani, G., 2006b. Using environmental tracers to assess groundwater resources in reclamation areas of Egypt. Geophysical Research Abstracts 8, A-05515.

Aeschbach-Hertig, W., El-Gamal, H., Dahab, K., Friedrich, R., Kipfer, R., Hajdase, I., 2007. Identifying and dating the origin of groundwater resources in reclamation areas of Egypt. Advances in Isotope Hydrology and its Role in Sustainable Water Resources Management. International Atomic Energy Agency (IAEA), Vienna, pp. 395–403.

Almogi-Labin, A., Bar-Matthews, M., Ayalon, A., 2004. Climate variability in the Levant and northeast Africa during the Late Quaternary based on marine and land records. In: Goren-Inbar, N., Speth, J.D. (Eds.), Human Paleoecology in the Levantine Corridor. Oxbow Press, Oxford, pp. 117–134.

Alsharhan, A.S., Salah, M.G., 1996. Geologic setting and hydrocarbon potential of North Sinai, Egypt. Bulletin of Canadian Petroleum Geology 44, 615–631.

Bar-Matthews, M., Ayalon, A., Gilmour, M., Matthews, A., Hawkesworth, C.J., 2003. Sea–land oxygen isotopic relationships from planktonic foraminifera and speleothems in the Eastern Mediterranean region and their implication for paleorainfall during interglacial intervals. Geochimica et Cosmochimica Acta 67, 3181–3199.

Bartov, Y., Stein, M., Enzel, Y., Agnon, A., Reches, Z., 2002. Lake levels and sequence stratigraphy of Lake Lisan, the late Pleistocene precursor of the Dead Sea. Quaternary Research 57, 9–21.

Bartov, Y., Goldstein, S.L., Stein, M., Enzel, Y., 2003. Catastrophic arid episodes in the east Mediterranean linked with the Atlantic Heinrich events. Geology 31, 439–442.

Bar-Yosef, O., Meadow, R., 1995. The origins of agriculture in the Near East. In: Price, T.D., Gebauer, A.B. (Eds.), The Last Hunters—First Farmers: Perspectives on the Prehistoric Transition to Agriculture. School of American Research Press, Santa Fe, New Mexico, pp. 39–94.

Blasband, B., White, S., Brooijmans, P., De Boorder, H., Visser, W., 2000. Late Proterozoic extensional collapse in the Arabian–Nubian Shield. Journal of the Geological Society of London 157, 615–628.

Bond, G., Broecker, W., Johnson, S., McManus, J., Labeyrie, L., Jouzel, J., Bonani, G.B., 1993. Correlation between climate records from North Atlantic sediments and Greenland ice. Nature 365, 507–508.

Brookes, I.A., 2003. Geomorphic indicators of Holocene winds in Egypt's Western Desert. Geomorphology 56, 155–166.

Cherkinsky, A.E., Culp, R.A., Dvoracek, D.K., Noakes, J.E., 2010. Status of the AMS facility at the University of Georgia. Nuclear Instruments and Methods in Physics Research 268, 867–870.

Clark, P.U., Dyke, A.S., Sakun, J.D., Carlson, A.E., Clark, J., Wohlfarth, B., Mitrovica, J.X., Hostetler, S.W., McCabe, A.M., 2009. The last glacial maximum. Science 325, 710–714.

Coplen, T.B., 1996. New guidelines for reporting stable hydrogen, carbon, and oxygen isotope-ratio data. Geochimica et Cosmochimica Acta 60, 3359–3360.

Craig, H., 1961. Isotopic variations in meteoric waters. Science 133, 1702–1703.

Edmunds, W.M., Fellman, E., Goni, I.B., 1999. Lakes, groundwater and paleohydrology in the Sahel of NE Nigerai: evidence from hydrogeochemistry. Journal of the Geological Society of London 156, 45–355.

Egyptian Meteorological Authority (EMA), 1996. Climatic Atlas of Egypt. Egyptian Meteorological Authority, Ministry of Transport and Communications, Cairo, Egypt.

Fairbanks, R.G., Mortlock, R.A., Chiu, T.-C., Cao, L., Kaplan, A., Guilderson, T.P., Fairbanks, T.W., Bloom, A.L., Grootes, P.M., Nadeau, M.-J., 2005. Radiocarbon calibration curve spanning 0 to 50,000 years BP based on paired $^{230}Th/^{234}U/^{238}U$ and ^{14}C dates on pristine corals. Quaternary Science Reviews 24, 1781–1796.

Fontes, J.-C., Garnier, J.-M., 1979. Determination of the initial ^{14}C activity of the total dissolved carbon: a review of the existing models and a new approach. Water Resources Research 15, 399–413.

Frumkin, A., Ford, D.C., Schwarcz, H.P., 2000. Paleoclimate and vegetation of the last glacial cycles in Jerusalem from a speleothem record. Global Biogeochemical Cycles 1, 1–9.

Gat, J.R., Mazor, E., Tzur, Y., 1969. The stable isotope composition of mineral waters in the Jordan Rift Valley, Israel. Journal of Hydrology 7, 334–352.

Geb, M., 2000. Factors favouring precipitation in North Africa: seen from the viewpoint of present-day meteorology. Global and Planetary Change 26, 85–96.

Gheith, H., Sultan, M., 2002. Construction of a hydrologic model for estimating wadi runoff and groundwater recharge in the Eastern Desert, Egypt. Journal of Hydrology 263, 36–55.

Guendouz, A., Moulla, A.S., Edmunds, W.M., Shand, P., Poole, J., Zouari, K., Mamou, A., 1998. Palaeoclimatic information contained in groundwater of the Grand ERG Orientale, North Africa. Isotope Techniques in the Study of Past and Current Environmental Changes in the Hydrosphere and Atmosphere. IAEA, Vienna, pp. 555–571.

Hesse, K.H., Hissese, A., Kheir, O., Schnacker, E., Schneider, M., Thorweihe, U., 1987. Hydrogeological investigations in the Nubian Aquifer system, Eastern Sahara. In: Kilitzsch, E., Schranck, E. (Eds.), Research in Egypt and Sudan. Dietrich Reimer, Berlin, pp. 397–464.

Himida, H., 1970. The Nubian artesian basin, its regional hydrogeological aspects and palaeohydrological reconstruction. Journal of Hydrology 9, 89–116.

International Atomic Energy Agency (IAEA), Water Isotope System for Data Analysis, Visualization, Electronic Retrieval (WISER), 2010. Water Isotope System for Data Analysis, Visualization, and Electronic Retrieval, 7th ed.

Issar, A., 2003. Climate Changes During the Holocene and their Impact on Hydrological Systems. Cambridge University Press, Cambridge, United Kingdom 144.

Issar, A., 2010. Climate change as a draw bridge between Africa and the Middle East. Global and Planetary Change 72, 451–454.

Issar, A., Zohar, M., 2004. Climate Change—Environment and Civilization in the Middle East. Springer, Berlin 252.

Issar, A., Bein, A., Michaeli, A., 1972. On the ancient water of the Upper Nubian Sandstone aquifer in central Sinai and southern Israel. Journal of Hydrology 17, 353–374.

Japan International Cooperation Agency (JICA), 1999. South Sinai Groundwater Resources Study in the Arab Republic of Egypt, Tokyo, Japan. 220.

Kipfer, R., Aeschbach-Hertig, W., Peeters, F., Stute, M., 2002. Noble gases in lakes and ground waters. In: Porcelli, D., Ballentine, C., Wieler, R. (Eds.), Reviews in Mineralogy and Geochemistry, Noble gases in Geochemistry and Cosmochemistry. Mineralogical Society of America and Geochemical Society, Washington, DC, pp. 615–700.

Klump, S., Tomonaga, Y., Kienzler, P., Kinzelbach, W., Baumann, T., Imboden, D.M., Kipfer, R., 2007. Field experiments yield new insights into gas exchange and excess air formation in natural porous media. Geochimica et Cosmochimica Acta 71, 1385–1397.

Lehmann, K.K., Berden, G., Engeln, R., 2009. An Introduction to Cavity Ring-Down Spectrometry. In: Berden, G., Engeln, R. (Eds.), Cavity Ring-Down Spectrometry Techniques and Applications. John Wiley & Sons Ltd., United Kingdom, pp. 1–26.

Lisker, S., Vaks, A., Bar-Matthews, M., Porat, R., Frumkin, A., 2009. Stromatolites in caves of the Dead Sea Fault Escarpment: implications to latest Pleistocene lake levels and tectonic subsidence. Quaternary Science Reviews 28, 80–92.

Manning, A.H., Solomon, D.K., 2003. Using noble gases to investigate mountain-front recharge. Journal of Hydrology 275, 194–207.

Mazor, E., 1972. Paleotemperatures and other hydrological parameters deduced from noble gases dissolved in groundwaters; Jordan Rift Valley, Israel. Geochimica et Cosmochimica Acta 36, 1321–1336.

National Climate Data Center (NCDC), 2012. Surface Data, Global Summary of the Day and Hourly Global. URL: http://www7.ncdc.noaa.gov/CDO/cdo.

Osmond, J.K., Dabous, A.A., 2004. Timing and intensity of groundwater movement during Egyptian Sahara pluvial periods by U-series analysis of secondary U in ores and carbonates. Quaternary Research 61, 85–94.

Parkhurst, D.L., Charlton, S.R., 2008. NetpathXL—An Excel® Interface to the Program NETPATH: U.S. Geological Survey Techniques and Methods 6–A26 (11 pp.).

Patterson, L.J., 2003. Chlorine-36 and stable chlorine isotopes in the Nubian Aquifer, Western Desert, Egypt. Earth and Environmental Sciences.University of Illinois, Chicago 81.

Pinti, D.L., Van Drom, E., 1988. PALEOTEMP: a Mathematica® program for evaluating paleotemperatures from the concentration of atmosphere-derived noble gases in groundwater. Computers & Geosciences 24, 33–41.

Plummer, L.N., Sprinkle, C.L., 2001. Radiocarbon dating of dissolved inorganic carbon in groundwater from confined parts of the Upper Floridan aquifer, Florida, USA. Hydrogeology Journal 9, 127–150.
Plummer, L.N., Michel, R.L., Thurman, E.M., Glynn, P.D., 1993. Environmental tracers for age dating young ground water. Regional ground-water quality.Van Nostrand Reinhold, New York 255–294.
Plummer, L.N., Prestemon, E.C., Parkhurst, D.L., 1994. An interactive code (NETPATH) for modeling net geochemical reactions along a flow path Version 2.0. U.S. Geological Survey Water-Resources Investigations Report 94–4169.
Prell, W.L., Kutzbach, J.E., 1987. Monsoon variability over the past 150,000 years. Journal of Geophysical Research 92, 8411–8425.
Rossignol-Strick, M., 1983. African monsoons, an immediate climate response to orbital insolation. Nature 304, 46–49.
Said, R., 1962. The Geology of Egypt. Elsevier, Amsterdam 377.
Said, R., 1971. Explanatory Notes to Accompany the Geological Map of Egypt. Geological Survey of Egypt, Cairo 123.
Sanford, W.E., 1997. Correcting for diffusion in carbon-14 dating of groundwater. Groundwater 35, 357–361.
Shata, A., 1982. Hydrogeology of the Great Nubian Sandstone basin, Egypt. Quarterly Journal of Engineering Geology 15, 127–133.
Solomon, D.K., Cook, P.G., Sanford, W.E., 1998. Dissolved gases in subsurface hydrology. In: Kendall, C., McDonnell, J.J. (Eds.), Isotope Tracers in Catchment Hydrology. Elsevier, Amsterdam, pp. 291–318.
Sonntag, C., Klitzsch, E., Lohnert, E.P., El Shazly, E.M., Munnich, K.O., Junghans, C., Thorweihe, U., Weistroffer, K., Swailem, F.M., 1978. Paleoclimatic Information from Deuterium and Oxygen-18 in Carbon-14-dated North Saharian groundwaters. Isotope Hydrology International Atomic Energy Agency (IAEA), Vienna 569–581.
Stern, R.J., Kroner, A., 1993. Late Precambrian crustal evolution in NE Sudan: isotopic and geochronologic constraints. Journal of Geology 101, 555–574.
Stuiver, M., Polach, H.A., 1977. Reporting of ^{14}C data. Radiocarbon 19, 355–363.
Sturchio, N.C., et al., 2004. One million year old groundwater in the Sahara revealed by krypton-81 and chlorine-36. Geophysical Research Letters 31, L05503.
Stute, M., Schlosser, P., 1993. Principles and applications of the noble gas paleo-thermometer. In: Swart, P.K., Lohmann, K.C., Savin, S. (Eds.), Climatic Change in Continental Isotopic Records. Geophysical Monograph Series. American Geophysical Union, pp. 89–100.
Stute, M., Clark, J.F., Schlosser, P., Broecker, W.S., 1995. A 30,000 yr continental paleotemperature record derived from noble gases dissolved in groundwater from the San Juan Basin, New Mexico. Quaternary Research 43, 209–220.
Sultan, M., Arvidson, R.E., Duncan, I.J., Stern, R.J., El Kaliouby, B., 1988. Extension of the Najd shear system from Saudi Arabia to the central Eastern Desert of Egypt based on integrated field and Landsat observations. Tectonics 7, 1291–1306.
Sultan, M., Sturchio, N., Hassan, F.A., Hamdan, M.A.R., Mahmood, A.M., El Alfy, Z., Stein, T., 1997. Precipitation source inferred from stable isotopic composition of Pleistocene groundwater and carbonate deposits in the Western Desert of Egypt. Quaternary Research 48, 29–37.
Sultan, M., Metwally, S., Milewski, A., Becker, D., Ahmed, M., Sauck, W., Soliman, F., Sturchio, N., Yan, E., Rashed, M., Wagdy, A., Becker, R., Welton, B., 2011. Modern recharge to fossil aquifers: geochemical, geophysical, and modeling constraints. Journal of Hydrology 403, 14–24.
Tamers, M.A., 1975. Validity of radiocarbon dates on groundwater. Geophysical Surveys 2, 217–239.
Thorweihe, U., 1990. Nubian aquifer system. In: Said, R. (Ed.), Geology of Egypt. Balkema, Rotterdam, pp. 601–611.
Torfstein, A., Goldstein, S.L., Stein, M., Enzel, Y., 2013. Impacts of abrupt climate changes in the Levant from last glacial Dead Sea levels. Quaternary Science Reviews 69, 1–7.
United States Geological Survey (USGS), 2003. USGS Global Visualization Viewer (GLOVIS). URL: http://glovis.usgs.gov.
Vaks, A., Bar-Matthews, M., Ayalon, A., Schilman, B., Gilmour, M., Hawkesworth, C.J., Frumkin, A., Kaufman, A., Matthews, A., 2003. Paleoclimate reconstruction based on the timing of speleothem growth and oxygen and carbon isotope composition in a cave located in the rain shadow in Israel. Quaternary Research 59, 139–284.
Vaks, A., Bar-Matthews, M., Ayalon, A., Matthews, A., Frumkin, A., Dayan, U., Halicz, L., Almogi-Labin, A., Schilman, B., 2006. Paleoclimate and location of the border between Mediterranean climate region and the Saharo–Arabian Desert as revealed by speleothems from the northern Negev Desert, Israel. Earth and Planetary Science Letters 249, 384–399.
Vogel, J.C., 1967. Investigation of groundwater flow with radiocarbon. Isotopes in Hydrology. International Atomic Energy Agency, Vienna, pp. 255–368.
Vogel, J.S., Southon, J.R., Nelson, D.E., Brown, T.A., 1984. Performance of catalytically condensed carbon for use in accelerator mass spectrometry. Nuclear Instruments and Methods in Physics Research Section B: Beam Interactions with Materials and Atoms 5, 289–293.
Weiss, R.F., 1968. Piggyback samplers for dissolved gas studies on sealed water samples. Deep-Sea Research 15, 695–699.
Yan, Z., Petit-Maire, N., 1994. The last 140 Ka in the Afro–Asian arid/semi-arid transitional zone. Palaeogeography, Palaeoclimatology, Palaeoecology 110, 217–233.

https://doi.org/10.1016/j.yqres.2013.10.017 Published online by Cambridge University Press